JOURNAL OF SOLID STATE CHEMISTRY **127,** 302–307 (1996)
ARTICLE NO. 0387

$(PO_2)_4(WO_3)_{14}$ Single Crystals of the $MPTB_p$ Family: A HREM Study

B. Domengès,[1] P. Roussel, Ph. Labbé, and D. Groult

Laboratoire CRISMAT-ISMRA, Bd. Maréchal Juin, 14050 Caen Cedex, France

Received May 3, 1996; in revised form September 4, 1996; accepted September 16, 1996

Electron microscopy study of crushed $m = 7$ $MPTB_p$ single crystals has been performed. In agreement with the X-ray diffraction structural results, these crystals exhibit a monoclinic symmetry and $P2_1/n$ space group. It was shown that whereas some single crystals appear very regular, others exhibit intergrowth defects with other members of the $MPTB_p$ family or with $MPTB_h$ slabs, which may badly influence electron transport behavior. © 1996 Academic Press

INTRODUCTION

Since their synthesis and structural characterization in the early 1980s (1–4), the monophosphate tungsten bronzes with pentagonal tunnels ($MPTB_p$), corresponding to the generic formulation $(PO_2)_4(WO_3)_{2m}$, have been extensively studied for their low-dimensional electronic properties leading to charge density wave (CDW) states (5–12). In $m = 4$ ($P_4W_8O_{32}$) and $m = 6$ ($P_4W_{12}O_{44}$) bronzes, two successive CDW transitions related to nesting properties of their Fermi surfaces have thus been characterized at low temperatures. In contrast, the CDW modulations observed for $m = 7$, 9, 10, and 11 bronzes present a large number of harmonics which are not well understood. Compared to even m members ($m = 4$, 6, 8), which have been the subject of detailed single crystal X-ray studies allowing the band structures to be established (13, 14), little is known about the actual structures of odd m members. Lately, the structure of the $m = 7$ ($P_4W_{14}O_{50}$) member has been investigated by X-ray single crystal diffraction and was shown to exhibit a monoclinic distortion (15) in contrast to the even m value counterparts ($m = 4$, 6, 8), which are orthorhombic. In order to get more information on the microstructure of the $m = 7$ crystals and the origin of this change in symmetry, a transmission electron microscopy study of $m = 7$ single crystals has been carried out. We report here the main results of this TEM investigation.

[1] To whom correspondence should be addressed.

EXPERIMENTAL

Platelike purple crystals of $P_4W_{14}O_{50}$ ($m = 7$) were prepared by chemical vapor transport, following a procedure reported elsewhere (15). Crystals were first identified by X-ray diffraction techniques and particularly using Weissenberg films. In order to characterize related crystals from the microscopic point of view, crystals were individually gently crushed in an agate mortar in *n*-butanol and deposited on a holey carbon-coated copper grid, so that fragments of only one crystal would be studied at a time. Two single crystals were investigated in this way. Electron diffraction (ED) was performed on a JEM200CX equipped with a tilting rotating goniometer ($\pm 60°$), which allows reciprocal space reconstruction, and the high resolution study on TOPCON 2B electron microscope equipped with a $\pm$ 10° double tilt goniometer and an objective lens with spherical aberration constant of 0.4 mm. Photographic enlargements of experimental images were scanned using a 600 dpi resolution scanner. High resolution image calculations (HREM) were performed using the multislice method of EMS package.

$P_4W_{14}O_{50}$: PREVIOUS STRUCTURAL STUDIES

$P_4W_{14}O_{50}$ is the $m = 7$ member of the series of the monophosphate tungsten bronzes with pentagonal tunnels ($MPTB_p$). Its structure is built up from mixed $(PO_2)(WO_3)_7(PO_2)$ slabs, i.e., ReO_3-type slabs whose width can be measured by the number of WO_6 octahedra (here seven) joined through PO_4 tetrahedra. At the junction, pentagonal tunnels are formed which are empty (Fig. 1). A previous electron microscopy study had been performed on powder samples (3) and the $m = 7$ member, like all other odd members ($m \geq 7$), appeared to crystallize with orthorhombic symmetry with cell parameters $a \approx 5.3$ Å, $b \approx 6.56$ Å, $c \approx 26.65$ Å. Lately, an accurate X-ray diffraction structural study on a single crystal evidenced a slight monoclinic ($\beta = 90.19°$) distortion of the cell, too small to be detected on ED patterns. Reflection conditions (hkl, no; $h0l$, $h + l = 2n$; $0k0$, $k = 2n$) lead to the space group $P2_1/n$. Electron

0022-4596/96 $18.00

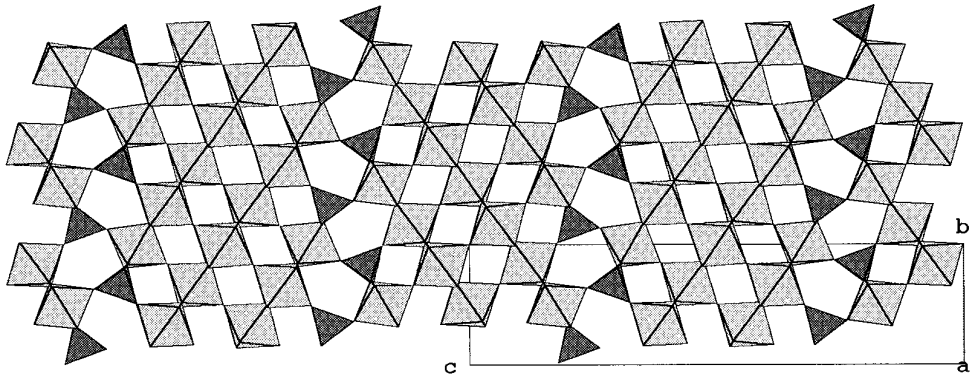

FIG. 1. [100] projection of the crystal structure of the $m = 7$ member of the $MPTB_p$ series.

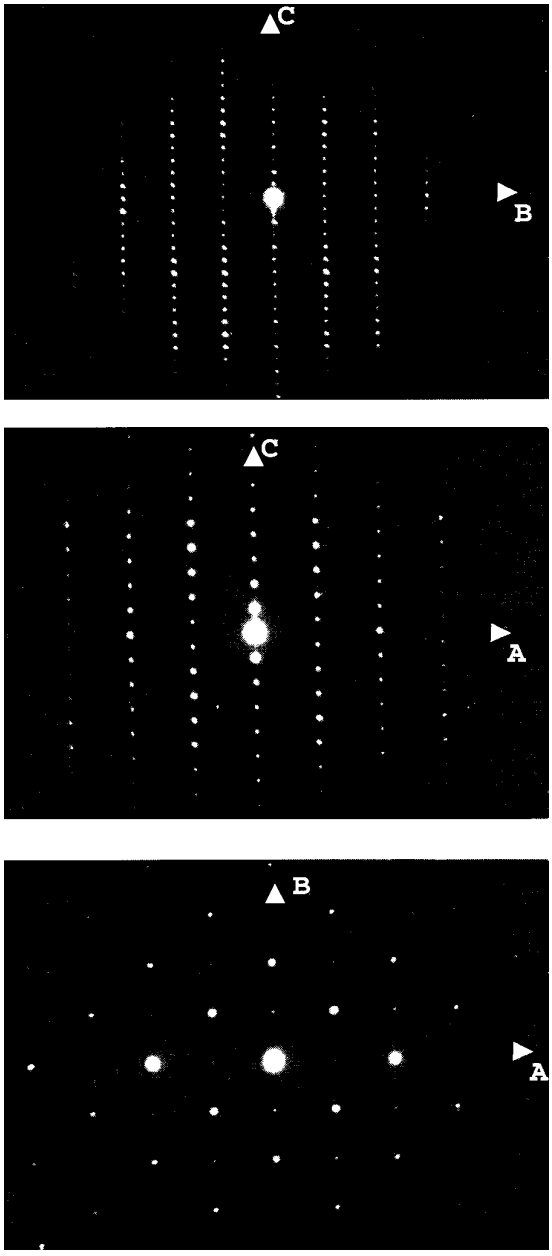

FIG. 2. [100], [010], and [001] ED patterns showing the reflection conditions: $0kl$, no; $h0l$, $h + l = 2n$; $hk0$, no. The observed $0k0$, $k = 2n + 1$ spots are due to multiple diffraction.

microscopy study of single crystals chosen from the same batch as that studied by X-ray diffraction appeared of interest trying to characterize under the microscopic point of view and to clarify the change of symmetry from even members (orthorhombic) to the odd $m = 7$ member (monoclinic). Furthermore, X-ray diffraction results are very similar to those recently obtained on the isostructural $(Mo, W)_9O_{25}$ compound (16, 17).

ELECTRON MICROSCOPY STUDY

The single crystal used to perform the structural study by X-ray diffraction was crushed to be studied by electron microscopy. Ten fragments were characterized by electron diffraction and six by HREM. The electron diffraction study agrees with the X-ray diffraction study concerning the symmetry and the reflection conditions. The presence of the screw axis parallel to **b** is confirmed and the $0k0$ spots with odd k values on ED patterns in Fig. 2 are due to double diffraction phenomena. Though the monoclinic distortion could hardly be measured, the raising of extinction conditions leading to the monoclinic symmetry was

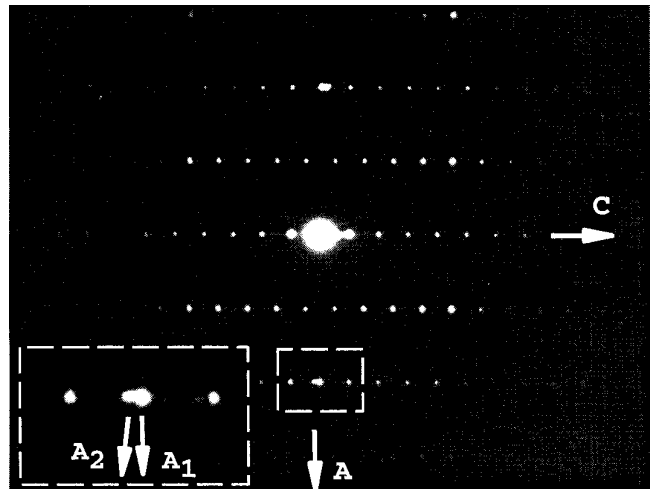

FIG. 3. [010] ED pattern showing splitting of dots parallel to **C**.

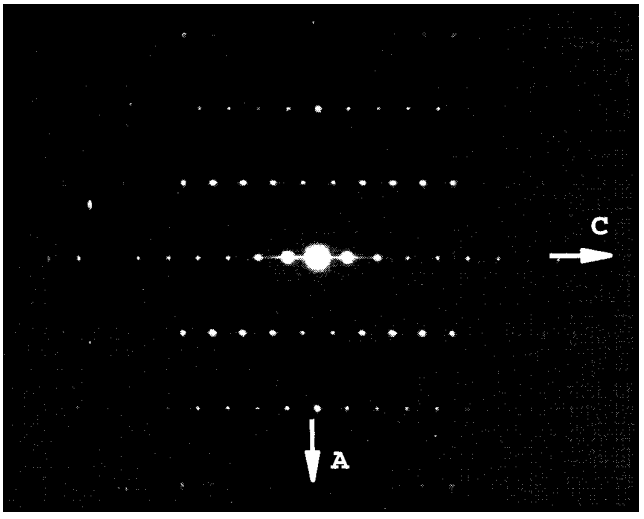

FIG. 4. [010] ED pattern showing diffuse streaks parallel to **C**.

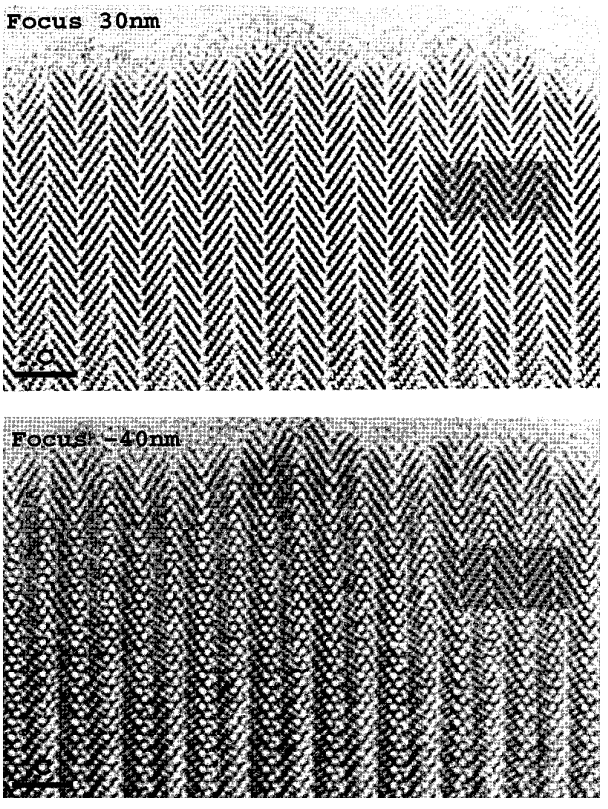

FIG. 5. Two typical [100] HREM images; calculated images are inset. (Calculation parameters are high-voltage $V = 200$ kV, objective aperture radius $R = 10$ nm^{-1}, spherical aberration constant $C_s = 0.4$ mm, spread of focus $\Delta = 10$ nm, beam semiconvergence $\alpha = 0.85$ mrad, crystal thickness $T = 4.2$ nm).

clearly observed (Fig. 2), though $hk0$, $h + k = 2n + 1$ spots are rather weak. As in the X-ray study, splitting of spots in [010] ED patterns parallel to **C** (Fig. 3) was often observed, which suggests twinning phenomena parallel to the direct **(a, b)** plane. Two fragment ED patterns exhibited slight diffuse streaks parallel to **C**, (Fig. 4), corresponding to intergrowth defects, i.e., other terms of the series, which would appear then to be rather scarce in the matrix.

Six fragments were investigated by high resolution electron microscopy. They all appeared very regular. The most representative projection of the structure is [100] (Fig. 5). The observed contrasts, which were previously described (4), do not fundamentally evolve with the resolution gain as shown from image calculations. Also, for low thicknesses, contrasts are better described in terms of dark contrast than in terms of bright contrast. Indeed, one can observe zig-zag ribbons of dark dots which, depending on the focus value, can be related either to the tungsten atoms or to the perovskite-type tunnels of the zig-zag ribbons of WO_6 octahedra. Figure 5 shows two typical focus value [100] images. In the 30 nm focus image, high electron density zones are highlighted so that bright ribbons are related to tungsten and oxygen atoms of the equatorial plane of the WO_6 octahedra and big bright dots in zig-zag patterns parallel to **b** correspond to the PO_4 tetrahedra. Big dark dots in zig-zag patterns parallel to **b** will then be related to the pentagonal tunnels and the ribbon of dark dots to

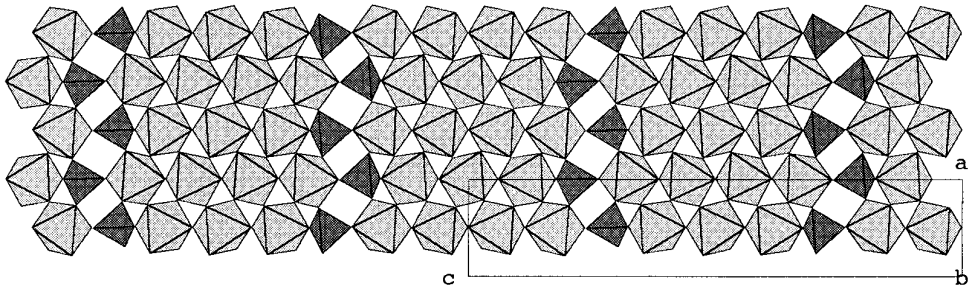

FIG. 6. [010] projection of $P_4W_{14}O_{50}$ crystal structure.

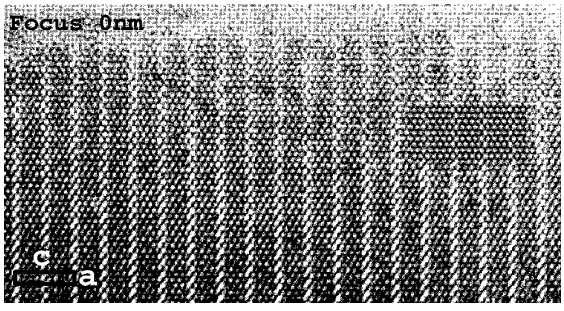

FIG. 7. Typical [010] HREM image and inset calculated image (crystal thickness $T = 3.9$ nm).

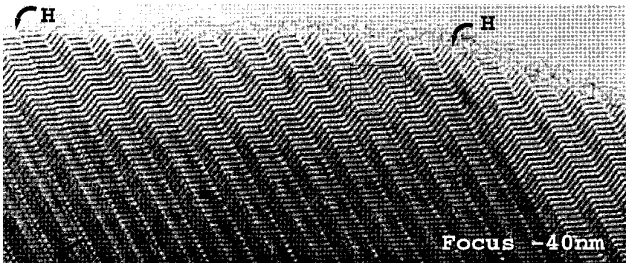

FIG. 9. [110] HREM image and inset calculated image (crystal thickness $T = 3.4$ nm). Two rows of hexagonal tunnels are observed (**H**).

the oxygen apices of the WO_6 octahedra. In the -40 nm focus image, low electron density zones are highlighted and bright ribbons are related to the perovskite type tunnels. Big dark dots forming ribbons in zig-zag patterns can be assigned to the oxygen apices of the WO_6 octahedra.

The [010] projection gives information on the regularity of the intergrowth but also on the regularity of the phosphate groups stacking along the **a** direction (Fig. 6). Indeed, defects such as translation of the phosphate plane perpendicular to the **a** axis were observed in the monophosphate tungsten bronzes with hexagonal tunnels, $MPTB_h$ (18). Here, the fragments observed along this direction show a very regular contrast (Fig. 7). The focus is close to 0 nm. High electron density zones are highlighted and tungsten atoms and phosphate groups appear as bright dots. The latter form zig-zag chains parallel to **a** and between these, one can count along **a** groups of three dots alternating with groups of four dots (i.e., three octahedra alternating with four octahedra). But also, following a line parallel to **c**, one can count a group of three bright dots, a diffuse bright dot, a group of four bright dots, and a diffuse bright one, i.e., three octahedra, one phosphate group, four octahedra, and one phosphate group, which reflect the periodicity of the structure (Fig. 6).

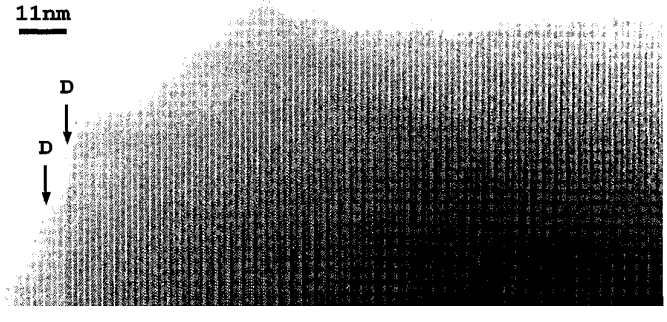

FIG. 8. Low magnification HREM [100] image showing only two intergrowth defects (**D**).

DEFECTS

Intergrowth defects were very rarely observed. As a quantification, along the **c** direction no more than two intergrowth defects (intergrowth with another member of the family) were observed on domains as large as 0.2 μm and they would occur at the boundary between domains (Fig. 8).

Intergrowth defects with a member of the family of the $MPTB_h$ were observed twice on one fragment (Fig. 9). The observation direction is [110]. Focus is close to -40 nm and low electron density zones are highlighted. Bright zig-zag lines are related to the perovskite-type tunnels and pentagonal tunnels viewed along [110], the latter being imaged through brighter big dots on the lines. Two very large slabs can be distinguished. Big bright dots can be seen nearly at the middle of the line which here slightly deviates. By comparison with previous observations on the $MPTB_h$ compounds, it appears most probable that the latter bright dots can be related to hexagonal tunnels, i.e., to an extra monophosphate planes which does not induce a change in the direction of the octahedron ribbon (Fig. 10).

The study of another crystal than the one used for the structure determination by X-ray diffraction showed that perfect crystals such as the previous one are not common. Indeed, most ED patterns of fragments of this second crystal showed diffuse streaks parallel to **c** indicative of intergrowth defects. As an example, the [010] image of Fig. 11 shows a modulation of contrast related to steps on the crystal and almost 10 defective slabs in 0.6 μm, that is, 10 times the previous crystal.

CONCLUSION

An electron microscopy study of $P_4W_{14}O_{50}$ single crystals was performed. It was shown that the change to monoclinic symmetry from the orthorhombic symmetry of even m members ($m = 4, 6, 8$) is not related to intergrowth or other structural defects but to intrinsic characteristics of the structure of the seventh member of the family, which

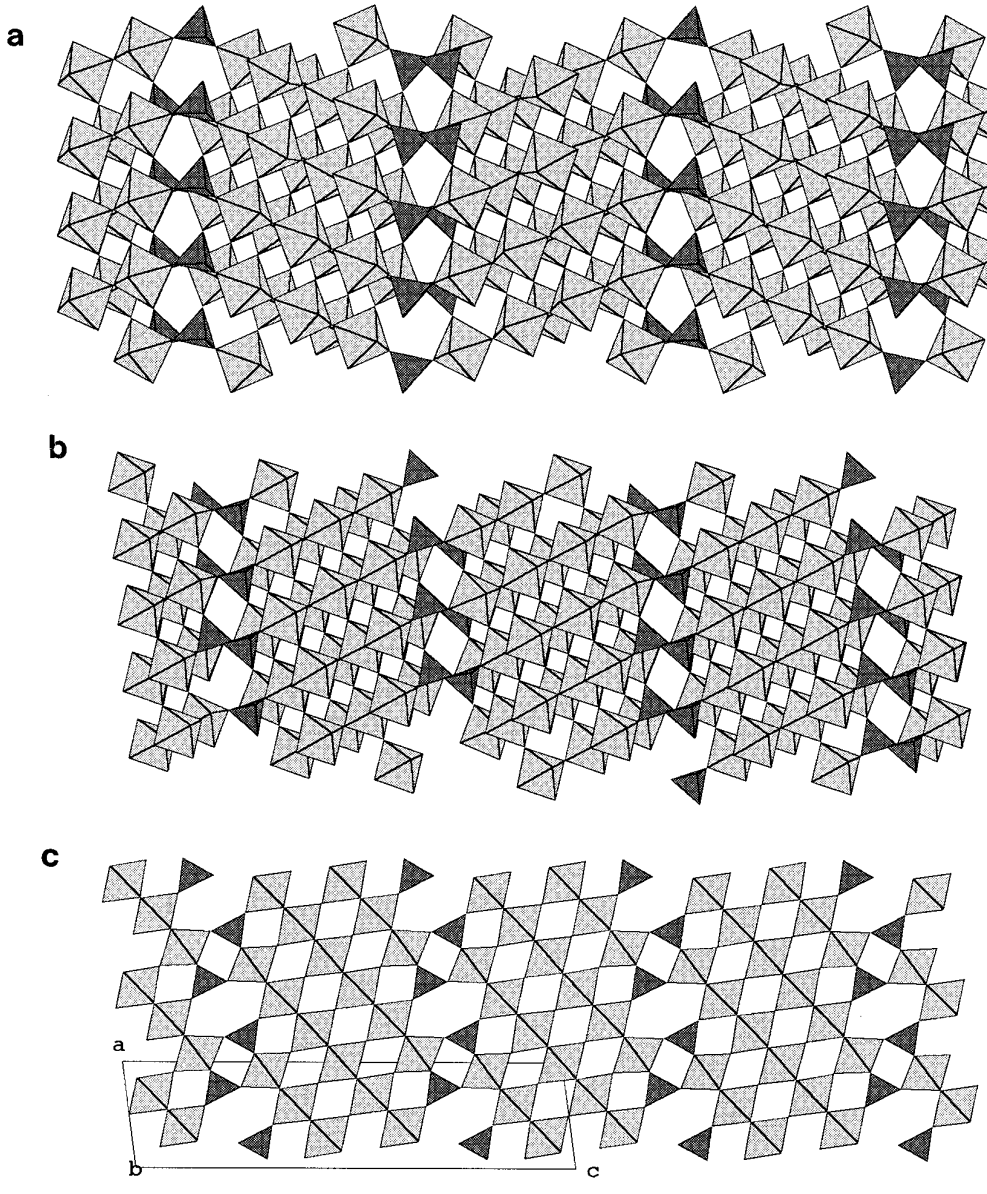

FIG. 10. [110] projection of $m = 7$ members of (a) $MPTB_p$ and (b) $MPTB_h$ structures. (c) [010] projection of $m = 7$ $MPTB_h$ structure (cation sites in the hexagonal tunnels are omitted).

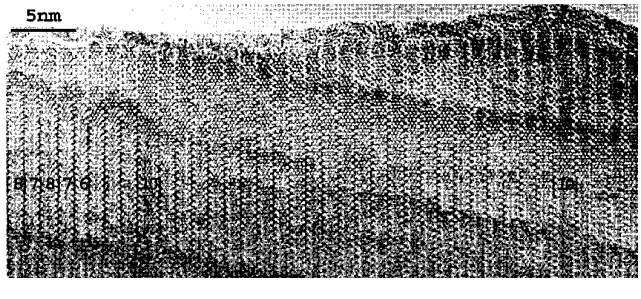

FIG. 11. Medium magnification of [010] HREM image showing several defective slabs; corresponding m values are given.

had previously been characterized by X-ray diffraction. The quality of the single crystals is a major problem and some single crystals will exhibit defects such as intergrowths which may influence their physical properties badly.

REFERENCES

1. J. P. Giroult, M. Goreaud, Ph. Labbé and B. Raveau, *Acta Crystallogr. Sect. B* **37,** 2139 (1981).
2. Ph. Labbé, M. Goreaud, and B. Raveau, *J. Solid State Chem.* **61,** 324 (1986).
3. A. Benmoussa, Ph. Labbé, D. Groult, and B. Raveau, *J. Solid State Chem.* **44,** 318 (1982).
4. B. Domengès, M. Hervieu, B. Raveau, and R. J. D. Tilley, *J. Solid State Chem.* **54,** 10 (1984).
5. Z. S. Teweldemedhin, K. V. Ramanujachary, and M. Greenblatt, *Phys. Rev. B* **46,** 7897 (1992).
6. E. Wang, M. Greenblatt, E. I. Rachidi, E. Canadell, M. H. Whangbo, and S. Vadlamannati, *Phys. Rev. B* **39,** 12969 (1989).
7. P Foury and J. P. Pouget *Int. J. Mod. Phys. B* **7,** 3973 (1993), and references therein.
8. P. Foury, J. P. Pouget, Z. S. Teweldemedhin, E. Wang, M. Greenblatt, and D. Groult, *J. Phys. IV C2* **3,** 133 (1993).
9. A. Ottolenghi, P. Foury, J. P. Pouget, Z. S. Teweldemedhin, M. Greenblatt, D. Groult, J. Marcus, and C. Schlenker, *Synth. Met.* **70,** 1301 (1995).
10. Y. Yan, M. Kleman, C. Le Touze, J. Marcus, C. Schlenker, and P. A. Buffat *Europhys. Lett.* **30,** 49 (1995).
11. A. Rötger, J. Lehman, C. Schlenker, J. Dumas, J. Marcus, Z. S. Teweldemedhin, and M. Greenblatt, *Europhys. Lett.* **25,** 23 (1994).
12. C. Le Touze, G. Bonfait, C. Schlenker, J. Dumas, M. Almeida, M. Greenblatt, and Z. S. Teweldemedhin, *J. Phys. I* **5,** 437 (1995), and references therein.
13. M. H. Whangbo, E. Canadell, P. Foury, and J. P. Pouget, *Science* **252,** 96 (1991).
14. E. Canadell and M. H. Whangbo, *J. Solid State Chem.* **86,** 131 (1990).
15. P. Roussel, Ph. Labbé, D. Groult, B. Domengès, H. Leligny, and D. Grebille, *J. Solid State Chem.* **122,** 281–290 (1996).
16. L. Kihlborg, B. O. Marinder, M. Sundberg, F. Portemer, and O. Ringaby, *J. Solid State Chem.* **111,** 111–117 (1994).
17. O. G. D'Yachenko, V. V. Tabachenko, and M. Sundberg, *J. Solid State Chem.* **119,** 8–12 (1995).
18. B. Domengès, M. Hervieu, B. Raveau, and M. O'Keeffe, *J. Solid State Chem.* **72,** 155 (1988).